Journal of Physics and Its Applications

Journal homepage : https://ejournal2.undip.ac.id/index.php/jpa/index

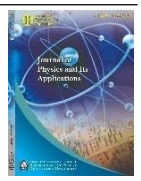

MEMS-Based Bridge Modal Frequency Identification Using FFT Averaging and Konno–Ohmachi Smoothing

Kholis Nurhanafi[1]*, Retno Deby Ayu Widia Ningtias[1], Ahmad Zarkasi[1], Devina Rayzy P.S.P[1], Auliya Rahmatul Ummah[1], Sri Wigantono[2], and Aditya Yoga Purnama[3]

[1]*Department of Physics, Faculty of Mathematics and Natural Sciences, Universitas Mulawarman, Samarinda, Indonesia*
[2]*Department of Mathematics, Faculty of Mathematics and Natural Sciences, Universitas Mulawarman, Samarinda, Indonesia*
[3]*Physics Education Department, Universitas Sarjanawiyata Tamansiswa, Yogyakarta, Indonesia*

**Corresponding author: kholis.nh@fmipa.unmul.ac.id*

ARTICLE INFO

Article history:
Received: 7 December 2025
Accepted: 5 February 2026
Available online: 30 May 2026

Keywords:
MEMS accelerometer
Ambient vibration
Modal frequency identification
FFT averaging
Konno–Ohmachi smoothing

ABSTRACT

Bridge structures undergo continuous degradation due to traffic loading and environmental exposure, necessitating the development of practical methods to monitor changes in their dynamic response. This study examines the use of a low-cost MEMS accelerometer for identifying dominant modal frequency bands (natural-frequency candidates) of an operational short-span bridge under ambient excitation. An ADXL345 sensor, integrated with an Arduino-based data acquisition system and a MATLAB interface, was used to record tri-axial vibration signals at three locations on the Jembatan Jalan Gelatik in Samarinda during both daytime and late-afternoon traffic conditions. The time-domain signals were processed using Welch's averaged windowed Fast Fourier Transform, followed by Konno–Ohmachi smoothing to clarify local spectral peaks. The analysis was intentionally limited to frequencies below 20 Hz, where global modes are expected, and the signal-to-noise ratio of the MEMS sensor is more reliable. Several consistent modal frequency bands were identified across measurement points, with dominant peaks observed between approximately 1.3–1.5 Hz, 2.1–2.7 Hz, 3.3–3.5 Hz, 5.0–6.8 Hz, 8.0–9.0 Hz, and 14–18 Hz. These peaks were validated through spatial repeatability across measurement points and temporal repeatability across different traffic conditions (daytime and late afternoon). These results indicate that the combination of low-cost sensing and noise-robust spectral processing can extract stable modal information from ambient bridge vibrations, despite the limitations of single-sensor deployment and the absence of reference-grade instruments. The findings suggest that this approach offers a feasible preliminary method for vibration-based structural assessment and may serve as a foundation for further development toward more detailed modal characterization.

1. Introduction

Bridges are essential components of transportation infrastructure, yet their structural condition inevitably deteriorates over time. Their service life is progressively shortened by the combined effects of increasing traffic loads and aggressive environmental conditions. Heavy and frequent traffic accelerates material fatigue, cracking, and reduction in load-bearing capacity, particularly in reinforced and prestressed concrete bridges [1], [2], [3]. Environmental factors, such as freeze–thaw cycles, moisture, rainfall, extreme temperatures, and chloride exposure in coastal regions or de-icing salt applications, further exacerbate reinforcement corrosion and concrete degradation [4], [5]. The interaction between traffic-induced fatigue and corrosion can reduce the expected lifespan of bridges by up to 70% in high-traffic areas exposed to aggressive climates [6], [7], [8]. These conditions underscore the importance of continuous monitoring to ensure safety and extend the lifespan of infrastructure services.

Monitoring a bridge's natural frequency is an effective and widely adopted method for evaluating its structural integrity. The natural frequency acts as a dynamic "fingerprint," and minor variations can indicate the presence of damage, degradation, or changes in boundary conditions. Because natural frequency is governed by structural stiffness and mass, a loss of stiffness arising from cracking, corrosion, or foundation scouring results in a measurable decrease in frequency [9], [10], [11]. Numerous laboratories, numerical, and field studies have demonstrated that reductions in natural frequency are reliable indicators of stiffness loss across concrete, steel, and historical bridge typologies [12], [13]. Continuous frequency monitoring is also crucial in mitigating the risk of resonance. Resonance between a bridge's natural frequency and dynamic excitations from pedestrians, traffic, trains, wind, or seismic activity can produce excessive vibrations that accelerate structural deterioration and, in severe cases, lead to collapse [14], [15], [16].

Structural Health Monitoring (SHM) has emerged as the standard approach for identifying such changes,

and conventional SHM deployments rely heavily on high-precision piezoelectric and force-balance accelerometers. Although highly accurate, these systems incur substantial limitations. First, high-grade accelerometers and their associated acquisition hardware are expensive and labor-intensive to install, which restricts large-scale deployment to flagship infrastructure with significant funding [17], [18]. Second, wired configurations are challenging to scale into dense sensing networks due to the complexity of cabling and maintenance demands [19]. Third, traditional sensors typically consume considerable power and require frequent maintenance, which limits their suitability for long-term, real-time monitoring [17]. As a result, continuous SHM has so far been limited to a small proportion of major bridges, while smaller and older bridges, which are often the most vulnerable, remain largely unmonitored. This situation creates a compelling need for low-cost and scalable alternatives.

Recent advancements in Micro-Electro-Mechanical Systems (MEMS) sensing technology, including the ADXL345 accelerometer, offer promising opportunities due to their compact size, low power consumption, and low cost. Despite these advantages, MEMS sensors exhibit a relatively high noise floor and lower sensitivity, which makes the extraction of true vibration signatures considerably more challenging compared to precision-grade accelerometers [20], [21].

Quantitatively, this limitation has been reported in multiple comparative studies. Feriadi *et al.* evaluated vibration measurements using the ADXL345 against a piezoelectric accelerometer (Vibroport 80) and found that ADXL345 consistently produced slightly higher acceleration amplitudes by approximately 3% (0.03–0.04 m/s^2) under various test conditions [22]. Hu *et al.* benchmarked a MEMS seismic sensor against a high-precision force-balance accelerometer (BL-03) and reported substantially lower self-noise for the force-balance unit, with an RMS noise of only 0.00088 cm/s^2 within the 0.1–20 Hz bandwidth [23]. Moreover, recent SHM-oriented sensor evaluations indicate that the noise density of low-cost MEMS accelerometers (typically hundreds of $\mu g/\sqrt{\text{Hz}}$) is orders of magnitude higher than the reference level required for SHM-grade accelerometers (often < 1 $\mu g/\sqrt{\text{Hz}}$), which may mask small-amplitude vibrations under low excitation. Nevertheless, Ribeiro *et al.* showed that despite higher noise levels, MEMS-based frequency estimates can still agree with professional piezoelectric instrumentation with frequency errors below approximately 1% when appropriate spectral processing techniques are applied [20].

Standard Fast Fourier Transform (FFT) techniques often struggle to distinguish between structural modal peaks, spectral leakage, and stochastic noise, particularly under ambient excitation conditions typical of operational bridges [24], [25]. Previous studies have introduced alternative modal identification approaches, such as robust time-domain parameter identification [26], Experimental Modal Analysis [27], and Power Spectral Density estimation using Welch's method [20]. More recent work has investigated hybrid techniques that integrate FFT, PSD, and Stochastic Subspace Identification [28]. However, the combination of Welch's Averaged Windowed FFT with Konno–Ohmachi smoothing, specifically targeted at improving modal peak stability from MEMS-based measurements, has not yet been systematically investigated for natural frequency extraction in bridges.

To address this gap, the present study implements a signal-processing workflow that integrates Welch's Averaged Windowed FFT with Konno–Ohmachi smoothing. The Averaged Windowed FFT method reduces the variance of spectral estimation by segmenting the signal into overlapping windows and averaging their periodograms, which improves peak consistency under noisy conditions [29], [30]. Konno–Ohmachi smoothing is then applied to suppress high-frequency fluctuations while preserving the sharpness and amplitude of genuine low-frequency structural modes, resulting in improved modal interpretability using low-sensitivity sensors [31], [32], [33]. To ensure reliable acquisition of time-domain vibration data prior to spectral processing, a custom MATLAB Graphical User Interface (GUI) was developed to facilitate communication between the ADXL345 accelerometer and an Arduino Uno microcontroller. The GUI enables configuration of sampling parameters, real-time visualization, and automated storage of analog voltage data for subsequent frequency analysis.

This research presents the design and validation of a low-cost, high-reliability SHM system capable of reliably identifying dominant natural-frequency candidates (modal frequency bands) in operational civil infrastructure, particularly bridges. The proposed system integrates MEMS accelerometers with a microcontroller-based acquisition platform and a dedicated MATLAB-based GUI. The spectral analysis workflow, which combines the Averaged Windowed FFT method and the Konno–Ohmachi smoothing technique, is designed to overcome the primary limitations of MEMS-based vibration measurements. The overall objective of the system is to enable scalable, affordable, and reliable vibration-based monitoring for transportation infrastructure with constrained maintenance budgets.

2. Method

2.1. System Overview

The proposed system is designed to perform vibration-based monitoring of bridge structures with the objective of identifying their natural frequencies using a low-cost sensing platform. The overall architecture follows an acquisition–processing workflow that transforms ambient structural vibration into natural frequency information. The workflow is illustrated in Figure 1 (System Workflow), which consists of four primary stages: (i) vibration sensing, (ii) data acquisition, (iii) signal processing, and (iv) frequency extraction.

In the first stage, ambient vibrations on the bridge surface are measured using an ADXL345 MEMS accelerometer positioned at selected locations along the span. The accelerometer transduces structural vibration into electrical signals corresponding to tri-axial acceleration. In the second stage, the Arduino Uno microcontroller serves as the data acquisition unit, digitizing the accelerometer output and transmitting the time-domain vibration data to a host computer via serial communication. This embedded

sensing and acquisition configuration enables compact field deployment as a low-cost alternative for bridge vibration measurements. Previous studies have reported that ADXL345-based sensing nodes can provide sufficiently reliable vibration measurements for SHM applications when proper calibration and acquisition procedures are applied [34], [35], [36].

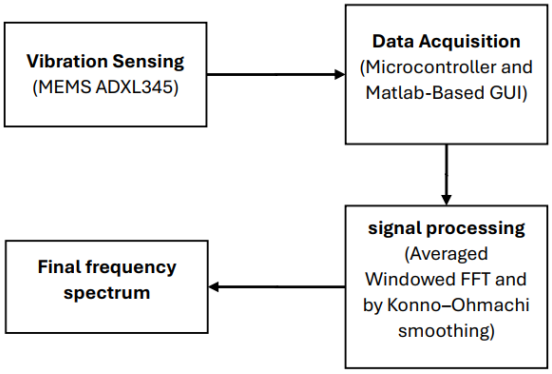

Fig. 1: System workflow

The third stage of the workflow occurs within the software environment through a custom MATLAB-based Graphical User Interface (GUI). The GUI allows the operator to configure sampling parameters, initiate and terminate data logging, visualize real-time acceleration input, and store the raw signal for further analysis. The final stage of the workflow is the signal processing chain, where the recorded acceleration data are converted into the frequency domain using a hybrid spectral method consisting of Welch's averaged windowed FFT , followed by Konno–Ohmachi smoothing [30], [31]. This combination is designed to improve the stability of modal peak identification when using low-sensitivity MEMS sensors under ambient excitation.

2.2. Hardware Design

The hardware platform consists of the ADXL345 MEMS accelerometer, an Arduino Uno microcontroller, and an independent power module. The complete arrangement is illustrated in Figure 2, showing the communication pathway between the sensing module, acquisition unit, and host computer. This configuration is designed to provide a compact and low-cost solution for in-service bridge vibration monitoring.

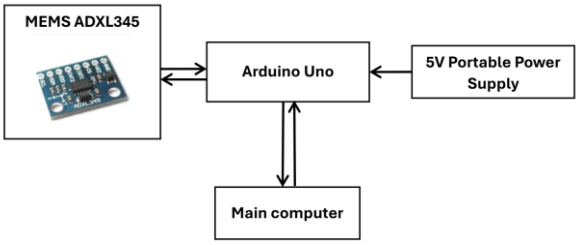

Fig. 2: Hardware design

The ADXL345 is selected due to its suitability for detecting low-amplitude vibrations. It is a tri-axial MEMS accelerometer with a configurable full-scale measurement range of ±2 g to ±16 g and a resolution of up to 13 bits, enabling reliable capture of ambient vibration responses [37], [38], [39]. The sensor communicates with the Arduino Uno via the I^2C interface [40], [41], and the microcontroller streams the digitized acceleration samples to the host computer through a serial link. The sampling rate is controlled by MATLAB GUI during the acquisition phase to maintain synchronized logging across all three axes.

For field deployment, the ADXL345 module is attached directly to the bridge deck using high-strength adhesive tape, providing sufficient contact for vibration transfer without requiring permanent modification to the structure. A portable 5 V power bank supplies both the accelerometer and the microcontroller, enabling untethered operation and eliminating the need for on-site electrical infrastructure. This hardware arrangement is designed for practical vibration measurements on operational bridges with low implementation cost.

2.3. Data Acquisition System

A custom MATLAB Graphical User Interface (GUI) was developed to facilitate the acquisition of vibration data from the ADXL345 accelerometer through the Arduino Uno microcontroller. The GUI provides the operator with essential controls for configuring sampling parameters, specifying measurement duration, and initializing communication with the acquisition unit. The complete layout of the GUI is shown in Figure 3.

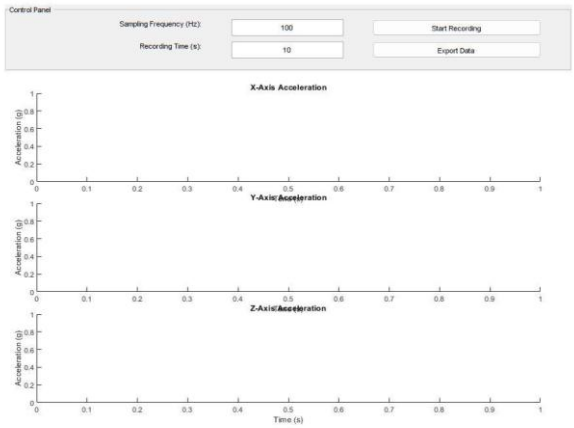

Fig. 3: Layout of the GUI

Once the measurement session begins, the GUI receives tri-axial acceleration samples from the Arduino via serial communication. A real-time plot of the incoming signal is displayed to allow on-site verification of sensor response and signal quality prior to data storage.

The ADXL345 data stream was acquired at a nominal sampling frequency of 100 Hz. The sampling interval was implemented in the Arduino acquisition loop using a 10 ms delay between successive samples, while the ADXL345 output configuration follows the default setting of the Adafruit ADXL345 library (ODR = 100 Hz). With this configuration, the Nyquist frequency is 50 Hz, which is sufficient for the present study that restricts frequency-domain analysis to below 20 Hz. Serial transmission between Arduino and MATLAB was performed at a baud rate of 9600 bps, and each sample was transmitted as three floating-point acceleration values (X, Y, Z) separated by delimiters. It is noted that the use of a low baud rate may introduce buffering-related latency during continuous tri-axial streaming at the nominal sampling rate. Nevertheless, since the analysis focuses on recurring dominant frequency bands

below 20 Hz extracted from long-duration recordings, the potential influence of occasional latency on peak-band identification is expected to be limited.

At the end of each acquisition run, the collected acceleration data are automatically saved in text format, preserving the raw time-domain signal required for subsequent spectral analysis. The use of a dedicated GUI eliminates manual configuration steps and supports fast, repeatable measurements during field testing, making the system practical for routine monitoring of in-service bridges.

2.4. Experimental Setup

Field measurements were conducted on Jembatan Jalan Gelatik, Samarinda, to obtain vibration data under real operational conditions. The bridge remained open to traffic during testing to ensure that the recorded signals reflected its natural dynamic response. The ADXL345 accelerometer was attached directly to the bridge deck using adhesive material tape, allowing temporary and non-destructive installation.

Three measurement points were selected along the span, as illustrated in Figure 4, which presents a Google Earth Map overlay indicating the exact sensor positions. Sensor locations were selected to capture the spatial repeatability of dominant modal frequency bands along the span. Points 1 and 3 were positioned near both bridge ends (not directly on the support bearings), while Point 2 was located at mid-span. Although vibration amplitudes are generally higher near mid-span for bending-dominated modes, end locations remain useful to confirm whether dominant spectral peaks are repeatable across the span, supporting the spatial consistency validation adopted in this study. The accelerometer orientation was kept consistent across all measurements: the Z-axis was aligned vertically to capture the dominant bridge vibration component, and the X- and Y-axes recorded horizontal responses. At each location, data were recorded for 15 minutes at a sampling rate of 100 Hz.

Fig. 4: Measurement points on Jembatan Jalan Gelatik, Samarinda (Source: Google Earth)

To assess the response of the structure under different excitation levels, measurements were taken under high-traffic conditions during the daytime and low-traffic conditions in the late afternoon. In this study, the term ambient vibration refers to operational excitation acting on the bridge, primarily induced by passing vehicles and other environmental disturbances. Since this excitation is not controlled and its force time-history is not directly measured, the measurement follows an output-only approach commonly used in Operational Modal Analysis (OMA). The recorded acceleration signals therefore represent the structural response output, while the ambient traffic excitation functions as an unknown input. Natural frequencies are subsequently identified from dominant recurring peaks in the response spectrum [42], [43]. During each recording session, the MATLAB GUI displayed the incoming acceleration signal in real time to verify signal quality prior to data storage. After each session, the raw time-domain acceleration signals were saved in text format for subsequent spectral analysis.

2.5. Signal Processing Pipeline

The vibration signals recorded from the ADXL345 accelerometer were processed using a three-stage workflow consisting of preprocessing, Averaged Windowed Fast Fourier Transform (FFT), and Konno–Ohmachi smoothing. The overall workflow is illustrated in Figure 5, which presents the complete sequence from raw acceleration input to the final extraction of dominant modal frequencies.

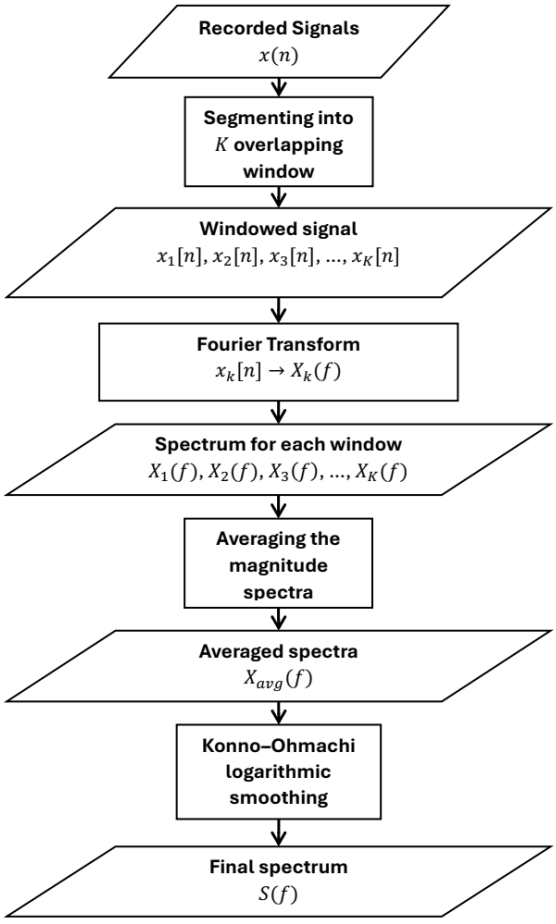

Fig. 5: Signal processing workflow

Let x[n] denote the discrete acceleration signal of length N samples. During preprocessing, each time series was trimmed to remove initial transients caused by sensor handling and then equalized in duration to ensure consistency across all measurement points and traffic conditions. No filtering was applied to maintain the integrity of low-amplitude modal components that may be relevant to bridge dynamics.

In the second stage, the trimmed signal was divided into K overlapping windows, each containing L samples. Each segment $x_k[n]$ was multiplied by a cosine-tapered window function w[n] and transformed to the frequency domain using the

Fourier Transform (FT). The magnitude spectrum $X_k(f)$ for each window was calculated as [30]:

$$X_k(f) = \left| \sum_{n=0}^{L-1} x_k[n] w[n] e^{-j2\pi fn/L} \right| \quad (1)$$

The magnitude spectra from all windows were then averaged to produce a noise-reduced and more stable representation of the frequency response [30].

$$X_{avg}(f) = \frac{1}{K} \sum_{k=1}^{K} X_k(f) \quad (2)$$

Averaging across the windowed FFTs reduces random spectral fluctuations and improves the visibility of modal peaks compared with a single FFT [30], [44].

In the final stage, the averaged spectrum was processed using Konno–Ohmachi logarithmic smoothing to enhance the interpretability of the dominant modal frequencies. The smoothed spectrum S(f) was computed as [31]:

$$S(f) = \frac{\sum_{i=1}^{M} X_{avg}(f_i) W(f, f_i)}{\sum_{i=1}^{M} W(f, f_i)} \quad (3)$$

where the smoothing kernel $W(f, f_i)$ is defined as

$$W(f, f_i) = \left[\frac{\sin\left(b \log_{10}\left(\frac{f}{f_i}\right)\right)}{b \log_{10}\left(\frac{f}{f_i}\right)} \right]^4 \quad (4)$$

In this formulation, f_i denotes the i -th discrete frequency bin of the averaged magnitude spectrum and M denotes the total number of frequency bins [31]. The parameter b controls the strength of smoothing. Large values of b retain sharp modal peaks, whereas small values result in heavier smoothing [45]. The logarithmic structure of the kernel preserves the shape and amplitude of dominant modal peaks, particularly in the low-frequency region associated with fundamental bridge modes, while attenuating high-frequency fluctuations caused by transient traffic events and sensor noise.

Natural frequencies were extracted by selecting dominant peaks in the smoothed spectrum. A modal candidate was accepted only if it appeared consistently across all sensing locations and under both traffic conditions, ensuring that noise artefacts were not misinterpreted as structural vibration modes.

2.6. Validation Strategy

The validation process examined whether the proposed low-cost monitoring system can extract natural frequencies reliably under real traffic conditions. Since no high-precision reference sensor was available for comparison, validation focused on assessing the internal consistency of the spectral results.

Validation was performed using two criteria applied exclusively to the Z-axis, which dominates the vertical vibration response of short- and medium-span bridges. First, spatial consistency was evaluated by comparing the smoothed spectra from the three sensor locations. A frequency peak was accepted as a modal-frequency candidate only when it appeared consistently at both ends of the bridge (Points 1 and 3) and at the mid-span (Point 2), even if peak amplitudes differed. This criterion is consistent with output-only Operational Modal Analysis (OMA) using peak-based identification (peak picking), where natural frequencies are estimated from recurring dominant peaks in vibration spectra under ambient excitation [46]. Second, temporal consistency was verified by comparing results from high-traffic (daytime) and low-traffic (late afternoon) measurements. A modal peak was considered valid only when its frequency remained stable across both excitation levels. Only frequency peaks satisfying both spatial and temporal consistency were interpreted as dominant modal frequency bands (estimated natural frequencies) of the bridge under ambient excitation.

3. Result and Discussion

3.1. Time-Domain Acceleration Responses

Figures 6, 7, and 8 present the Z-axis acceleration signals recorded at Points 1, 2, and 3 under daytime (high-traffic) and late-afternoon (low-traffic) conditions. The signals are dominated by a nearly constant offset that corresponds to the static gravity component of the MEMS accelerometer. The dynamic bridge response appears as small fluctuations superimposed on this offset.

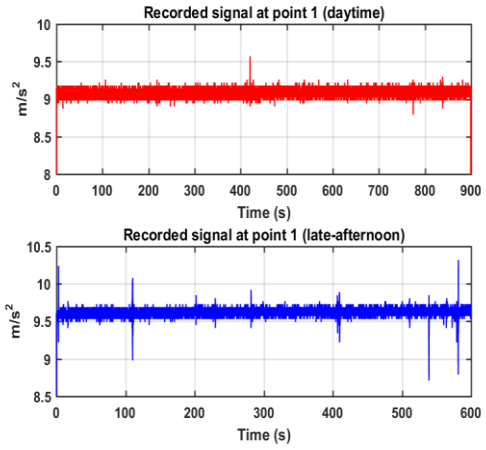

Fig. 6: Recorded signals at point 1

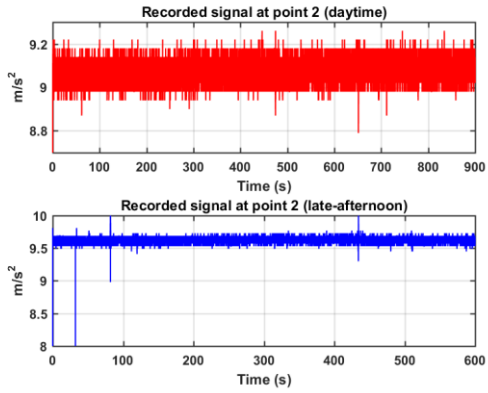

Fig. 7: Recorded signals at point 2

At Point 1, the daytime signal shows relatively small variations around the mean level, whereas the afternoon record contains several stronger transient fluctuations. At Point 2, the opposite behaviour is observed: the daytime signal exhibits higher variance across the full duration, while the afternoon record is

closer to a steady baseline. At Point 3, both daytime and afternoon signals show clearly visible vibration content throughout the measurement period. To provide quantitative support for the time-domain response, RMS and variance were computed for the Z-axis acceleration after removing the DC component associated with gravity, and the results are summarized in Table 1. Across all datasets, RMS values range from 0.058 to 0.268 m/s^2, with variances ranging from 0.0034 to 0.072 $(m/s^2)^2$. These non-zero metrics confirm that the recorded signals contain measurable dynamic vibration components under both traffic conditions. Therefore, the time-domain responses provide sufficient dynamic information for subsequent frequency-domain analysis and dominant peak identification, despite the limited sensitivity of the low-cost MEMS accelerometer.

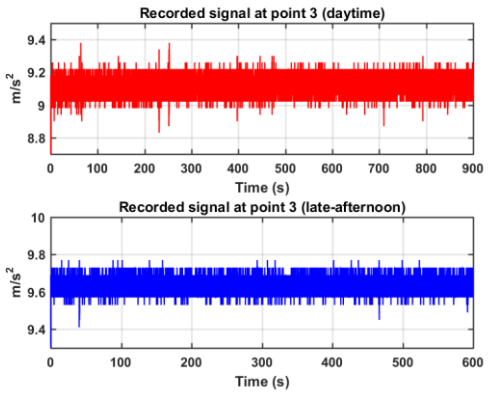

Fig. 8: Recorded signals at point 3

Table 1: RMS and variance for the Z-axis acceleration

Dataset	RMS (m/s^2)	Variance ($(m/s^2)^2$)
Point 1 - Daytime	0.26845	0.072067
Point 1 - Afternoon	0.068486	0.0046904
Point 2 – Daytime	0.058113	0.0033771
Point 2 – Afternoon	0.077858	0.0060619
Point 3 – Daytime	0.06024	0.0036289
Point 3 - Afternoon	0.064756	0.0041935

3.2. Frequency-Domain Analysis and Identification of Natural Frequencies

The averaged and smoothed spectra obtained from the Z-axis acceleration measurements at Points 1, 2, and 3 are presented in Figures 9, 10, and 11. Each figure contains two spectral curves corresponding to daytime and late-afternoon measurements, with local maxima annotated separately for each condition. Although the exact peak amplitudes and some of the peak positions differ between the two traffic conditions, the same frequency bands consistently contain dominant peaks across all measurement locations. his suggests that variations in traffic excitation mainly influence spectral magnitude, while the dominant modal frequency bands remain relatively stable across the measurement conditions. This trend is consistent with observations commonly reported in ambient vibration modal identification studies [13], [47], [48].

It should be noted that the spectra presented in Figures 9–11 correspond to processed results after FFT averaging and Konno–Ohmachi smoothing. These processing steps were necessary because the raw ambient vibration recordings were affected by practical field challenges, including uncontrolled traffic excitation, variations in peak prominence across recordings, and the relatively high noise floor of the MEMS sensor. By stabilizing the spectral estimate and reducing high-frequency fluctuations, the adopted workflow improved the interpretability of modal peaks under operational conditions.

At Point 1, the daytime spectrum shows peaks at approximately 0.80 Hz, 1.40 Hz, 2.70 Hz, 6.80 Hz, 11.10 Hz, and 17.80 Hz. The late-afternoon recording produces peaks at 2.20 Hz, 3.10 Hz, 5.00 Hz, 9.00 Hz, and 18.70 Hz. While the values do not numerically coincide, many of these peaks occur within similar modal regions, particularly around 1–3 Hz, 5–7 Hz, 9–12 Hz, and 17–19 Hz. These recurring bands suggest that Point 1 successfully captured a representative subset of the global vibration modes.

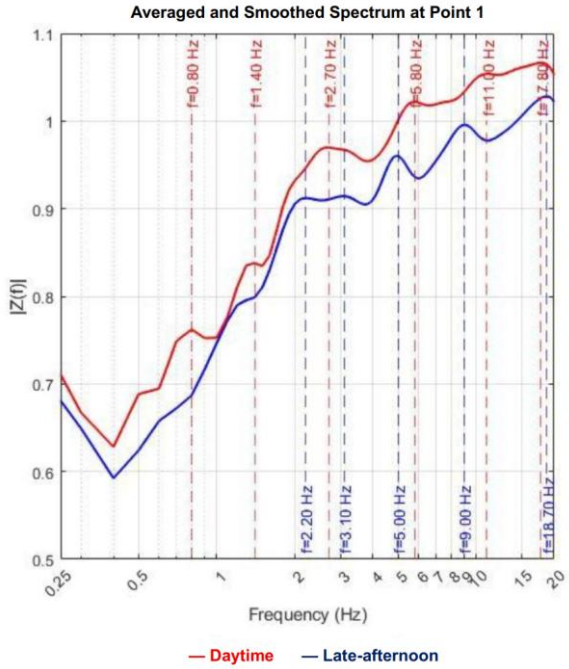

Fig. 9: Final spectrum for point 1

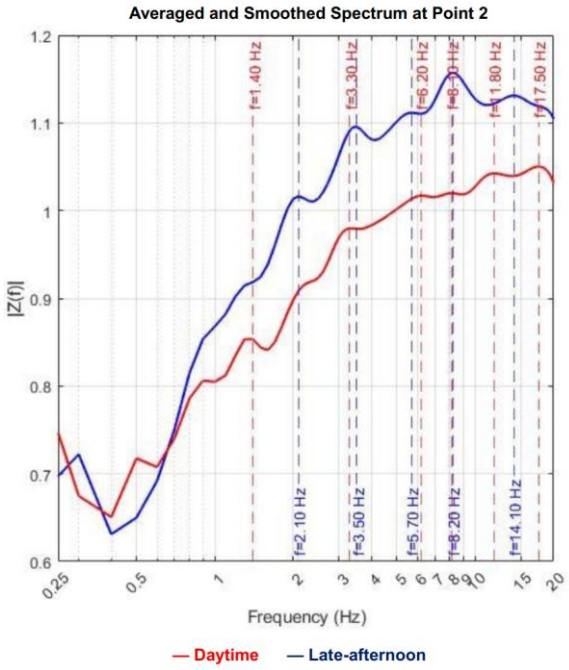

Fig. 10: Final spectrum for point 2

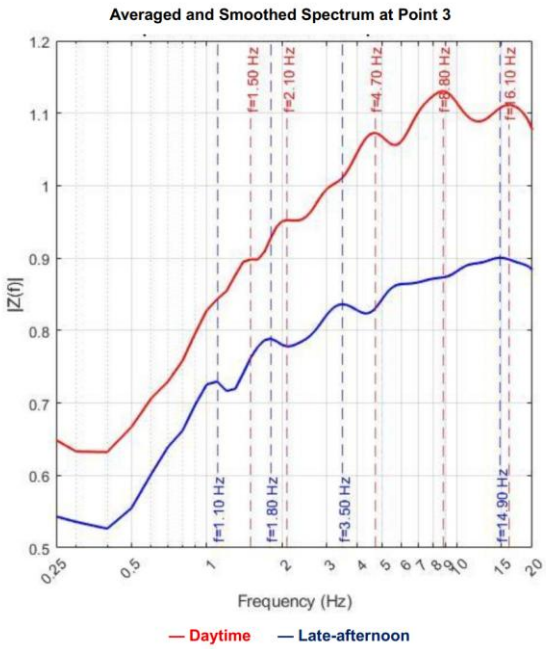

Fig. 11: Final spectrum for point 3

At Point 2, the daytime spectrum contains peaks at 1.40 Hz, 3.30 Hz, 6.20 Hz, 8.10 Hz, 11.80 Hz, and 17.50 Hz. The afternoon spectrum exhibits peaks near 2.10 Hz, 3.50 Hz, 5.70 Hz, 8.20 Hz, and 14.10 Hz. Compared with the daytime measurement, the late-afternoon spectrum shows more clearly separated peaks and improved peak contrast, indicating that modal signatures are more distinctly resolved under lower and more intermittent traffic excitation. This observation is consistent with previous studies reporting that bending-related modal responses are often more observable around mid-span locations [49], [50], [51]. However, the degree of peak separation and prominence remains dependent on the variability and broadband characteristics of ambient traffic excitation, which can reduce spectral contrast during high-traffic conditions. The recurrence of peaks around 1–2 Hz, 3–4 Hz, 5–7 Hz, and approximately 8 Hz further reinforces the stability of these modes.

At Point 3, the daytime spectrum exhibits peaks around 1.50 Hz, 2.10 Hz, 4.70 Hz, 8.80 Hz, and 16.10 Hz, while the afternoon spectrum reveals peaks at approximately 1.10 Hz, 1.80 Hz, 3.50 Hz, and 14.90 Hz. The low-frequency range (1.10–1.50 Hz) is particularly well-defined at this location, which aligns with the expectation that sensor positions near the bridge ends are more sensitive to boundary-condition influences, resulting in a stronger expression of the lower modes.

Taken together, the three measurement locations exhibit a set of recurring modal regions despite variations in excitation amplitude and ambient noise. Based on spatial and temporal consistency, six dominant modal frequency bands were identified (presented in Table 2). These bands represent the natural frequencies most reliably observed across all spectra and form the basis for subsequent validation and interpretation of the bridge's dynamic behavior.

The modal frequency bands identified from the spectra show consistent structural responses across all three measurement points. The first two modes, located between 1.3–1.5 Hz and 2.1–2.7 Hz, appear in both daytime and afternoon measurements and represent the most stable features of the bridge's vibration behavior. These frequencies fall within the range commonly reported for the fundamental vertical modes of short- to medium-span reinforced concrete bridges subjected to ambient traffic excitation [52], [53], [54]. The modes in the mid-frequency range, specifically around 3.3–3.5 Hz and 5.0–6.8 Hz, are visible across all locations, although their prominence varies depending on traffic conditions and sensor position. Higher-frequency peaks near 8–9 Hz and 14–18 Hz also appear consistently across the bridge, but with greater variation in amplitude, likely due to ambient noise and the reduced sensitivity of the MEMS sensor at higher frequencies. Despite these variations, the repeated appearance of the same frequency bands at different points and under different excitation levels indicates that they represent the dominant natural frequencies of the structure. This consistency suggests that the proposed system can support the identification of dominant modal frequency bands under low-amplitude ambient vibration.

Table 2: Dominant Modal Frequency Bands Identified from All Measurement Points

Mode	Natural Frequency (Hz)	Justification
f_1	1.30–1.50 Hz	Present at Points 1, 2, and 3 during both daytime and afternoon recordings.
f_2	2.10–2.70 Hz	Appears consistently in all locations with slight shifts due to ambient excitation variability.
f_3	3.30–3.50 Hz	Most clearly expressed at Point 2 (mid-span), indicating bending-mode sensitivity.
f_4	5.00–6.80 Hz	Detected at all points; amplitudes influenced by traffic conditions.
f_5	8.00–9.00 Hz	Recurring peak region associated with higher-order bending or local deck effects.
f_6	14.00–18.00 Hz	Visible across all points, though with stronger expression at the ends (Points 1 and 3).

3.3. Implications and Limitations

The findings of this study demonstrate that a low-cost MEMS-based system, when combined with FFT averaging and Konno–Ohmachi smoothing, is capable of consistently identifying natural frequency bands from ambient bridge vibrations. The recurring peaks observed across the three measurement points indicate that the signal-processing workflow is effective in stabilizing spectral features, even under low-amplitude excitation. These results demonstrate the potential of using accessible, low-cost instrumentation for preliminary vibration assessment in field settings where high-grade structural monitoring equipment may not be available. The integrated system, comprising an ADXL345 accelerometer, an Arduino data acquisition unit, and a MATLAB interface for signal processing, further demonstrates the feasibility of deploying compact and easily operated tools for practical bridge monitoring activities.

To support the rigor of the extracted modal frequency bands, validation was performed using an

internal consistency approach. Specifically, dominant peaks were accepted only when they appeared consistently across the three measurement locations and remained within the same frequency bands under both daytime (high-traffic) and late-afternoon (low-traffic) conditions. Quantitative time-domain metrics (RMS and variance) of the Z-axis signals (Table 1) further confirm measurable dynamic vibration content in all recordings. Since no reference-grade accelerometers were available during field deployment, the assessment focuses on repeatability and internal consistency rather than absolute accuracy.

Several limitations must be acknowledged. First, the analysis was intentionally restricted to frequencies below 20 Hz, since this range typically contains the dominant global vibration modes of short-span bridges and provides the most reliable information when using low-cost sensors. This methodological boundary helps reduce the influence of high-frequency noise, but also means that possible higher-order modes above 20 Hz were not investigated. Second, ambient traffic excitation introduces variability in spectral amplitudes, causing some peaks to appear more prominently in certain recordings than others. Third, the use of a single sensor at a time prevents simultaneous multi-point measurements, which limits the analysis to modal frequency identification rather than allowing estimation of complete mode shapes. Additionally, the study does not include comparison with reference-grade accelerometers, so the results represent internally consistent findings rather than externally validated modal parameters.

Overall, the outcomes suggest that low-cost MEMS sensing, combined with noise-robust spectral analysis, can provide reliable estimates of dominant modal frequencies under operational conditions. Further work involving controlled excitation, multi-sensor deployment, and higher-grade reference instrumentation would strengthen the system's applicability for more detailed structural evaluation.

4. Conclusion

This study demonstrated that a low-cost vibration monitoring system, based on a MEMS ADXL345 accelerometer, an Arduino acquisition platform, and an FFT-averaging spectral workflow with Konno–Ohmachi smoothing, can identify the dominant modal frequency bands of an operational short-span bridge using ambient excitation. Field measurements at three locations on Jembatan Jalan Gelatik yielded repeatable frequency bands between approximately 1.3 Hz and 18 Hz, indicating that the combined hardware and processing approach is capable of extracting stable modal information despite low-amplitude vibrations and sensor noise. The analysis was intentionally limited to frequencies below 20 Hz, where global modes are expected, and the sensor's signal-to-noise characteristics are more reliable. Although the method is limited to modal frequency identification and lacks simultaneous multi-point measurements or reference-grade validation, the results demonstrate that low-cost sensing, supported by noise-robust spectral analysis, can serve as an accessible starting point for preliminary structural vibration assessment. Future work may expand the system to include multi-sensor configurations, controlled excitation tests, and benchmarking against higher-grade accelerometers, enabling more detailed modal characterization.

Acknowledgment

The authors gratefully acknowledge the Faculty of Mathematics and Natural Sciences at Universitas Mulawarman for its institutional support. Appreciation is also extended to the Electronics and Instrumentation Physics Laboratory for providing the facilities and technical assistance required for this work. The authors also acknowledge the contributions of the students, lecturers, and staff of the Electronics and Instrumentation Physics Research and Study Group, whose support during data collection and field activities was crucial to the completion of this study.

References

[1] Y. Luo, H. Zheng, H. Zhang, and Y. Liu, "Fatigue reliability evaluation of aging prestressed concrete bridge accounting for stochastic traffic loading and resistance degradation," *Advances in Structural Engineering*, vol. 24, pp. 3021–3029, 2021, doi: 10.1177/13694332211017995.

[2] F. Pugliese, R. Risi, and L. Sarno, "Reliability assessment of existing RC bridges with spatially-variable pitting corrosion subjected to increasing traffic demand," *Reliab. Eng. Syst. Saf.*, vol. 218, p. 108137, 2021, doi: 10.1016/j.ress.2021.108137.

[3] M. Zizi, C. Chisari, and G. De Matteis, "Effects of pre-existing damage on vertical load-bearing capacity of masonry arch bridges," *Eng. Struct.*, p., 2024, doi: 10.1016/j.engstruct.2023.117205.

[4] M. Fujiu, T. Minami, and J. Takayama, "Environmental Influences on Bridge Deterioration Based on Periodic Inspection Data from Ishikawa Prefecture, Japan," *Infrastructures (Basel).*, p., 2022, doi: 10.3390/infrastructures7100130.

[5] S. H. Lee, L. An, and H.-K. Kim, "Risk-based bridge life cycle cost and environmental impact assessment considering climate change effects," *Sci. Rep.*, vol. 15, p., 2025, doi: 10.1038/s41598-024-82568-4.

[6] M. Borah and A. Sil, "Service-Life Estimation of a Reinforced Concrete Bridge Structure Exposed to Chloride-Contaminated Environments and Variable Traffic Loads," *ASCE. ASME. J. Risk Uncertain. Eng. Syst. A Civ. Eng.*, p., 2023, doi: 10.1061/ajrua6.rueng-1054.

[7] J. Su, J. Zhang, J. Zhou, C. Hu, and Y. Zheng, "Fatigue Life Assessment of Suspenders in Tied-Arch Bridges Under Random Traffic Loads and Environmental Corrosion," *International Journal of Civil Engineering*, vol. 21, pp. 523–540, 2022, doi: 10.1007/s40999-022-00792-3.

[8] D. Devendiran and S. Banerjee, "Influence of Combined Corrosion–Fatigue Deterioration on Life-Cycle Resilience of RC Bridges," *Journal of Bridge Engineering*, p., 2023, doi: 10.1061/jbenf2.beeng-5708.

[9] F. Reza, "A Simple Experiment in Structural Vibrations for Civil Engineering Students," *2022 ASEE Annual Conference &*

Exposition Proceedings, p., 2024, doi: 10.18260/1-2--40936.

[10] K. Kariyawasam, C. Middleton, G. Madabhushi, S. Haigh, and J. Talbot, "Assessment of bridge natural frequency as an indicator of scour using centrifuge modelling," *J. Civ. Struct. Health Monit.*, vol. 10, pp. 861–881, 2020, doi: 10.1007/s13349-020-00420-5.

[11] B. A. Aasim, A. Karimi, and J. Tomiyama, "Assessment of a Real-life Concrete Bridge Structure using Vibration-based Damage Detection Method," *IOP Conf. Ser. Mater. Sci. Eng.*, vol. 1054, p., 2021, doi: 10.1088/1757-899x/1054/1/012011.

[12] K. Maes, L. Meerbeeck, E. Reynders, and G. Lombaert, "Validation of vibration-based structural health monitoring on retrofitted railway bridge KW51," *Mech. Syst. Signal Process.*, p., 2022, doi: 10.1016/j.ymssp.2021.108380.

[13] S. S. Saidin *et al.*, "Vibration-based approach for structural health monitoring of ultra-high-performance concrete bridge," *Case Studies in Construction Materials*, p., 2022, doi: 10.1016/j.cscm.2022.e01752.

[14] Z. Wu, N. Zhang, J. Yao, and V. Poliakov, "Wavelet Time-Frequency Analysis on Bridge Resonance in Train-Track-Bridge Interactive System," *Applied Sciences*, p., 2022, doi: 10.3390/app12125929.

[15] P. Museros, E. Moliner, and M. Martínez-Rodrigo, "Free vibrations of simply-supported beam bridges under moving loads: Maximum resonance, cancellation and resonant vertical acceleration," *J. Sound Vib.*, vol. 332, pp. 326–345, 2013, doi: 10.1016/j.jsv.2012.08.008.

[16] T. Lu, B. Duan, B. Wang, and Z. Wang, "Brief Analysis of Natural Frequency and Its Corresponding Influences for Old Tacoma Narrows Bridge Using Finite Element Method," *Proceedings of the 7th International Conference on Architecture, Materials and Construction*, p., 2022, doi: 10.1007/978-3-030-94514-5_8.

[17] J. Villacorta-Calvo *et al.*, "Design and Validation of a Scalable, Reconfigurable and Low-Cost Structural Health Monitoring System," *Sensors (Basel).*, vol. 21, p., 2021, doi: 10.3390/s21020648.

[18] S. A. V. Shajihan, R. Chow, K. Mechitov, Y. Fu, T. Hoang, and B. Spencer, "Development of Synchronized High-Sensitivity Wireless Accelerometer for Structural Health Monitoring," *Sensors (Basel).*, vol. 20, p., 2020, doi: 10.3390/s20154169.

[19] F. Zonzini, M. Malatesta, D. Bogomolov, N. Testoni, A. Marzani, and L. De Marchi, "Vibration-Based SHM With Upscalable and Low-Cost Sensor Networks," *IEEE Trans. Instrum. Meas.*, vol. 69, pp. 7990–7998, 2020, doi: 10.1109/tim.2020.2982814.

[20] R. Ribeiro and R. Lameiras, "Evaluation of low-cost MEMS accelerometers for SHM: frequency and damping identification of civil structures," *Latin American Journal of Solids and Structures*, p., 2019, doi: 10.1590/1679-78255308.

[21] A. Elhattab, N. Uddin, and E. OBrien, "Extraction of Bridge Fundamental Frequencies Utilizing a Smartphone MEMS Accelerometer," *Sensors*, vol. 19, no. 14, p. 3143, Jul. 2019, doi: 10.3390/s19143143.

[22] I. Feriadi, F. Aswin, and M. Nugraha, "Analisis Sistem Pengukuran Getaran Mems Accelerometer ADXL345," *Manutech : Jurnal Teknologi Manufaktur*, p., 2019, doi: 10.33504/manutech.v9i02.48.

[23] X. Hu *et al.*, "Improved Resolution and Cost Performance of Low-Cost MEMS Seismic Sensor through Parallel Acquisition," *Sensors (Basel).*, vol. 21, p., 2021, doi: 10.3390/s21237970.

[24] T. Liu, H. Xu, M. Ragulskis, M. Cao, and W. Ostachowicz, "A Data-Driven Damage Identification Framework Based on Transmissibility Function Datasets and One-Dimensional Convolutional Neural Networks: Verification on a Structural Health Monitoring Benchmark Structure," *Sensors*, vol. 20, no. 4, p. 1059, Feb. 2020, doi: 10.3390/s20041059.

[25] T. Chen, Q. Wang, and X.-J. Yao, "High-resolution frequency domain decomposition for modal analysis of bridges using train-induced free-vibrations," *Advances in Structural Engineering*, vol. 27, no. 9, pp. 1528–1546, Jul. 2024, doi: 10.1177/13694332241252278.

[26] M. Omidalizarandi, R. Herrmann, B. Kargoll, S. Marx, J. Paffenholz, and I. Neumann, "A validated robust and automatic procedure for vibration analysis of bridge structures using MEMS accelerometers," *Journal of Applied Geodesy*, vol. 14, pp. 327–354, 2020, doi: 10.1515/jag-2020-0010.

[27] C. Bedon, E. Bergamo, M. Izzi, and S. Noè, "Prototyping and Validation of MEMS Accelerometers for Structural Health Monitoring - The Case Study of the Pietratagliata Cable-Stayed Bridge," *J. Sens. Actuator Networks*, vol. 7, p. 30, 2018, doi: 10.3390/jsan7030030.

[28] M. Crognale, C. Rinaldi, F. Potenza, V. Gattulli, A. Colarieti, and F. Franchi, "Developing and Testing High-Performance SHM Sensors Mounting Low-Noise MEMS Accelerometers," *Sensors (Basel).*, vol. 24, p., 2024, doi: 10.3390/s24082435.

[29] D.-J. Jwo, I.-H. Wu, and Y. Chang, "Windowing Design and Performance Assessment for Mitigation of Spectrum Leakage," *E3S Web of Conferences*, p., 2019, doi: 10.1051/e3sconf/20199403001.

[30] D.-J. Jwo, W. Chang, and I.-H. Wu, "Windowing Techniques, the Welch Method for Improvement of Power Spectrum Estimation," *Computers, Materials & Continua*, p., 2021, doi: 10.32604/cmc.2021.014752.

[31] K. Konno and T. Ohmachi, "Ground-motion characteristics estimated from spectral ratio between horizontal and vertical components

of microtremor," *Bulletin of the Seismological Society of America*, vol. 88, no. 1, pp. 228–241, Feb. 1998, doi: 10.1785/BSSA0880010228.

[32] X. Bian, Z. Shi, Y. Shao, Y. Chu, and X. Tan, "Variational Mode Decomposition for Raman Spectral Denoising," *Molecules*, vol. 28, p., 2023, doi: 10.3390/molecules28176406.

[33] L. Liu, Z. Wu, Z. Dong, and S. Yang, "Modal Identification of Low-Frequency Oscillations in Power Systems Based on Improved Variational Modal Decomposition and Sparse Time-Domain Method," *Sustainability*, p., 2022, doi: 10.3390/su142416867.

[34] S. U. Rehman, M. Usman, M. H. Y. Toor, and Q. A. Hussaini, "Advancing Structural Health Monitoring: A Vibration-Based IoT Approach for Remote Real-Time Systems," *Sens. Actuators A Phys.*, p., 2023, doi: 10.1016/j.sna.2023.114863.

[35] R. Concepcion, F. Cruz, F. Uy, J. M. Baltazar, J. Carpio, and K. Tolentino, "Triaxial MEMS digital accelerometer and temperature sensor calibration techniques for structural health monitoring of reinforced concrete bridge laboratory test platform," *2017IEEE 9th International Conference on Humanoid, Nanotechnology, Information Technology, Communication and Control, Environment and Management (HNICEM)*, pp. 1–6, 2017, doi: 10.1109/hnicem.2017.8269422.

[36] J. E. Rosal and M. Caya, "Development of Triaxial MEMS Digital Accelerometer on Structural Health Monitoring System for Midrise Structures," *2018 IEEE 10th International Conference on Humanoid, Nanotechnology, Information Technology,Communication and Control, Environment and Management (HNICEM)*, pp. 1–5, 2018, doi: 10.1109/hnicem.2018.8666311.

[37] A. Holovatyy, V. Teslyuk, M. Iwaniec, and M. Mashevska, "Development of a system for monitoring vibration accelerations based on the raspberry pi microcomputer and the ADXL345 accelerometer," *Eastern-European Journal of Enterprise Technologies*, vol. 6, pp. 52–62, 2017, doi: 10.15587/1729-4061.2017.116082.

[38] Y. Pramudya and M. Islamiah, "Vibration characteristics study on observatory using accelerometer ADXL345 sensor and Arduino," *THE 8TH NATIONAL PHYSICS SEMINAR 2019*, p., 2019, doi: 10.1063/1.5132658.

[39] N. N. Johari, F. Chee, S. R. M. Hashim, B. Golutin, and J. Dayou, "Descriptive Statistical Calibration Method of Triaxial Digital Accelerometer ADXL345 as Earthquakes Sensor," *Borneo Science | The Journal of Science and Technology*, p., 2023, doi: 10.51200/bsj.v44i1.4340.

[40] D. Kononov and Yu. Ostapchuk, "Development ff Measuring Complex for Determination of Kinematic Characteristics of Vibration Screen," *International scientific and technical conference Information technologies in metallurgy and machine building*, p., 2022, doi: 10.34185/1991-7848.itmm.2022.01.058.

[41] S. Salman, S. Sugiman, E. D. Sugiman, N. N. Sulistyowati, N. Sarah, and S. Salman, "Prototype of small-scale test machine for vibration measurement on bearings," *World Journal of Advanced Research and Reviews*, p., 2024, doi: 10.30574/wjarr.2024.24.2.3486.

[42] S. Russotto, V. Denoël, and A. Pirrotta, "An innovative only-output method to identify a structural system," *J. Phys. Conf. Ser.*, vol. 2647, p., 2024, doi: 10.1088/1742-6596/2647/22/222008.

[43] M. Davoodi, S. Mostafavian, S. Nabavian, and G. Jahangiri, "Output-only Modal Identification of beams with different boundary condition," *arXiv preprint,* p., 2023, doi: 10.48550/arXiv.2309.01719.

[44] M. Lamb and V. Rouillard, "Assessing the Influence of Fourier Analysis Parameters on Short-Time Modal Parameter Extraction," *J. Vib. Acoust.*, vol. 134, p. 31002, 2012, doi: 10.1115/1.4005654.

[45] M. Yazdi, R. Motamed, and J. Anderson, "A New Set of Automated Methodologies for Estimating Site Fundamental Frequency and Its Uncertainty Using Horizontal-to-Vertical Spectral Ratio Curves," *Seismological Research Letters*, p., 2022, doi: 10.1785/0220210078.

[46] H. Hasani and F. Freddi, "Operational Modal Analysis on Bridges: A Comprehensive Review," *Infrastructures (Basel).*, p., 2023, doi: 10.3390/infrastructures8120172.

[47] F. L. Zhang, H. B. Xiong, W. X. Shi, and X. Ou, "Structural health monitoring of Shanghai Tower during different stages using a Bayesian approach," *Struct. Control Health Monit.*, vol. 23, no. 11, pp. 1366–1384, Nov. 2016, doi: 10.1002/stc.1840.

[48] X. Zhi-Qian, P. Jian-Wen, W. Jin-Ting, and C. Fu-Dong, "Improved approach for vibration-based structural health monitoring of arch dams during seismic events and normal operation," *Struct. Control Health Monit.*, vol. 29, no. 7, Jul. 2022, doi: 10.1002/stc.2955.

[49] X.-Y. Pei, Y. Hou, H.-B. Huang, and J. Zheng, "A Multi-Objective Sensor Placement Method Considering Modal Identification Uncertainty and Damage Detection Sensitivity," *Buildings*, p., 2025, doi: 10.3390/buildings15050821.

[50] W. Xiang, J. Wei, and F. Zhang, "Structural Health Monitoring Design and Performance Evaluation of a Middle-Span Bridge," *Sensors (Basel).*, vol. 23, p., 2023, doi: 10.3390/s23218702.

[51] C. O'Higgins, D. Hester, P. McGetrick, E. Cross, W. Ao, and J. Brownjohn, "Minimal Information Data-Modelling (MID) and an Easily Implementable Low-Cost SHM System for Use on a Short-Span Bridge," *Sensors (Basel).*, vol. 23, p., 2023, doi: 10.3390/s23146328.

[52] P. Agarwal, P. Pal, and P. K. Mehta, "Free Vibration Analysis of RC Box-Girder Bridges

Using FEM," *Sound&Vibration*, p., 2022, doi: 10.32604/sv.2022.014874.
[53] I. Drygala and J. Dulińska, "Full-Scale Experimental and Numerical Investigations on the Modal Parameters of a Single-Span Steel-Frame Footbridge," *Symmetry (Basel).*, vol. 11, p. 404, 2019, doi: 10.3390/sym11030404.
[54] C. O'Higgins, D. Hester, P. McGetrick, E. Cross, W. Ao, and J. Brownjohn, "Minimal Information Data-Modelling (MID) and an Easily Implementable Low-Cost SHM System for Use on a Short-Span Bridge," *Sensors (Basel).*, vol. 23, p., 2023, doi: 10.3390/s23146328.